

## Article

# A Numerical Modeling Study of a New Type of Hydraulic Mechanical Continuously Variable Transmission (HMCVT) with Optimized Transmission Efficiency

Zexin Ma <sup>1</sup>, Zhengyu Li <sup>2</sup>, Deming Sun <sup>2</sup>, Yanbin Cai <sup>2</sup>, Jiwei Zhang <sup>2</sup>, Hongyu Liu <sup>1</sup>, Qingxin Wang <sup>1</sup>, He Li <sup>1</sup>, Long Zhou <sup>3</sup>, Wenbin Yu <sup>1,\*</sup>  and Feiyang Zhao <sup>1,\*</sup>

<sup>1</sup> School of Energy and Power Engineering, Shandong University, Jinan 250012, China; 202234544@mail.sdu.edu.cn (Z.M.); liuhongyu@mail.sdu.edu.cn (H.L.); 202320707@mail.sdu.edu.cn (Q.W.); 202214478@mail.sdu.edu.cn (H.L.)

<sup>2</sup> WeiChai Lovol Intelligent Agricultural Technology Co., Ltd., Weifang 261200, China; lizhengyu@lovol.com (Z.L.); sundeming@lovol.com (D.S.); caiyanbin@lovol.com (Y.C.); zhangjiwei1@lovol.com (J.Z.)

<sup>3</sup> AVL List Technical Center (Shanghai) Co., Ltd., Shanghai 201206, China; long.zhou@avl.com

\* Correspondence: wbyu@sdu.edu.cn (W.Y.); fyzhao@sdu.edu.cn (F.Z.)

**Abstract:** Hydraulic mechanical continuously variable transmission (HMCVT) is widely used in powerful tractors due to its excellent performance. This paper aims to find universal methods for analyzing and optimizing the transmission efficiency of HMCVT. The energy efficiency improvement of HMCVT is important for the economy of powerful tractors. Firstly, by correctly analyzing the transmission efficiency of HMCVT, the transmission efficiency during the operation of HMCVT can be accurately calculated. Secondly, an improved NSGA-II genetic algorithm was adopted to achieve dynamic optimization of shifting points through transmission parameter combination optimization, ensuring smooth shifting while improving overall transmission efficiency. According to the transmission efficiency simulation platform, the accuracy of the transmission efficiency calculation was verified. Adopting an improved NSGA-II genetic algorithm to continuously optimize the design of HMCVT configurations achieves dynamic optimization of HMCVT parameters without being limited by shifting speed. The specific HMCVT structure proposed in this study can meet the requirements of a three-speed continuously variable transmission at speeds of 0–50 km/h. Meanwhile, the improved NSGA-II genetic algorithm can effectively provide support for the design of various HMCVT powertrain systems.

**Keywords:** HMCVT; transmission efficiency; transmission parameter optimization algorithm; HMCVT efficiency simulation platform



Academic Editor: Mateusz Dybkowski

Received: 18 November 2024

Revised: 11 December 2024

Accepted: 2 January 2025

Published: 6 January 2025

**Citation:** Ma, Z.; Li, Z.; Sun, D.; Cai, Y.; Zhang, J.; Liu, H.; Wang, Q.; Li, H.; Zhou, L.; Yu, W.; et al. A Numerical Modeling Study of a New Type of Hydraulic Mechanical Continuously Variable Transmission (HMCVT) with Optimized Transmission Efficiency. *Designs* **2025**, *9*, 6. <https://doi.org/10.3390/designs9010006>

**Copyright:** © 2025 by the authors. Licensee MDPI, Basel, Switzerland. This article is an open access article distributed under the terms and conditions of the Creative Commons Attribution (CC BY) license (<https://creativecommons.org/licenses/by/4.0/>).

## 1. Introduction

With the rapid development of smart agriculture [1,2], high horsepower tractors play an important role as the main agricultural machinery driving agricultural production. The output torque and speed of the tractor transmission need to constantly update to adapt to changes with external loads [3]. In this background, the application of continuously variable transmissions has become a promising development trend. The most commonly used types of continuously variable transmissions (CVTs) are the hydraulic static transmission (HST) and the hydro-mechanical continuously variable transmission (HMCVT). Among these, the efficiency of hydraulic static transmissions (HSTs) is significantly lower than that of gear transmissions, limiting their widespread use in high-power tractors [4]. To

address the limitations of HSTs, an upgraded design incorporates a parallel connection with mechanical components, resulting in the development of the hydraulic-mechanical continuously variable transmission (HMCVT) [5,6]. The hydraulic part only transmits part of the power, and the remaining power is transmitted through mechanical components. As a result, transmission efficiency is enhanced, while also offering improved driving comfort [7,8].

The hydraulic mechanical continuously variable transmission began in the early 20th century. Due to limitations in the manufacturing level of hydraulic systems, HMCVT did not begin to be applied to vehicles until the 1960s [9]. The calculation accuracy of HMCVT efficiency has guiding significance for subsequent optimization designs. Jiang Li et al. proposed a novel method for analyzing the efficiency characteristics of variable loads, providing theoretical support for efficiency improvement in the design and analysis of multi-planet HMCVT tractors [10]. Zhang G et al. obtained the expression for the transmission efficiency of HMCVT composed of dual row planetary gears by analyzing torque, transmission ratio, and power cycling phenomena [11]. Lu Kai et al. proposed a method based on Variational Mode Decomposition (VMD), Particle Swarm Optimization (PSO), and Backpropagation (BP) neural network to improve the quality of transmission efficiency prediction, which can better adjust the transmission ratio during tractor operation [12]. It can be seen that an accurate evaluation of HMCVT is crucial for the design of HMCVT.

The transmission optimization design of HMCVT is important for improving the performance of high-power tractors. To improve the transmission efficiency of HMCVT, Cheng Z et al. used an improved genetic algorithm to determine the variable speed shift connection point. By changing the crossover and genetic probabilities in the genetic algorithm, the speed and accuracy of the algorithm were improved [13]. Afterwards, Cheng Z et al. improved the speed and accuracy of the HMCVT optimization algorithm by changing the crossover and genetic probabilities in the genetic algorithm [14]. Later, they established a tractor transmission model using a new five level HMCVT, which is characterized with more accurate efficiency. A segmented modeling method for HMCVT efficiency characteristics was referenced, which was based on an improved genetic algorithm [15]. Li J et al. designed an improved NSGA-II genetic algorithm based on system speed regulation, power performance, and economic characteristics [16]. The optimization design of HMCVT characteristic parameters was carried out with the goal of optimizing torque ratio and transmission efficiency. Finally, the torque ratio was increased by approximately 2.81%, 14.32%, 2.31%, and 15.07% in HM1, HM2, HM3, and HM4, respectively. Also, the transmission efficiency was increased by approximately 3.48% and 1.97% in HM1 (HM3) and HM2 (HM4).

In order to achieve an accurate evaluation of HMCVT efficiency and optimize transmission parameters based on transmission efficiency, this paper first proposes a new three-speed HMCVT scheme suitable for high horsepower intelligent tractors. The planetary gear adopts the Ravigneaux Hertz planetary gear structure, which has higher space utilization compared to the common Simpson planetary gear mechanism and can achieve multiple gears in relatively few components. Secondly, the transmission efficiency of the new HMCVT was calculated using the Крейнес method. Thirdly, based on the characteristics of comprehensive transmission efficiency and smooth shifting of all gears, an improved NSGA-II genetic algorithm was adopted, which combines simulated annealing and non-uniform mutation ideas. This algorithm achieves the dynamic optimization of HMCVT shift points and transmission parameters.

## 2. Theoretical Analysis on Transmission Characteristics of HMCVT

The HMCVT structure proposed in this paper is shown in Figure 1. It includes input shaft 1, the pump motor hydraulic system, Ravigneaux planetary gear mechanism, gear pair, shift clutch (C1, C2, C3), and directional clutch. The mechanical path runs from shaft 1 to shaft 3. The hydraulic path goes from shaft 1 to shaft 2, then from shaft 2 to shaft 4 and from shaft 4 to shaft 5. Finally, the mechanical transmission path and hydraulic transmission path are coupled and transmitted to shaft 6 in the planetary gear mechanism.

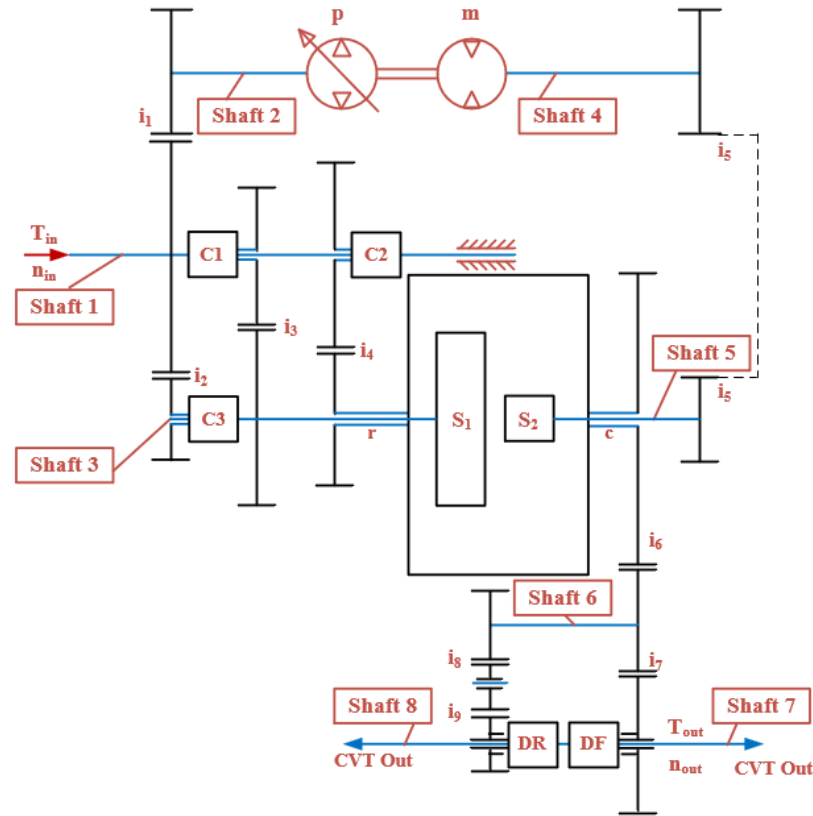


**Figure 1.** Schematic diagram of HMCVT for tractor. Note:  $i_1$  to  $i_9$  are gear ratios;  $k_1$  and  $k_2$  are characteristic parameters of Ravigneaux planetary gears; C1, C2, and C3 are first, second, and third gear clutches; DF and DR are forward and reverse gears; and  $n_{in}$  and  $T_{in}$  are input speed and torque, while  $n_{out}$  and  $T_{out}$  are output speed and torque.

### 2.1. Speed Characteristic

#### 2.1.1. Ranges HM1 and HM3

As illustrated in Figure 1, the engine output power is transmitted to HMCVT through shaft 1. The power transmission routes for the first and third gears are basically the same, except for gear pairs  $i_3$  and  $i_2$ . In both cases, in the Ravigneaux planetary gear system, the large sun gear  $S_1$  and the small sun gear  $S_2$  are inputs. The planetary carrier  $c$  is the output.  $n_{in}$  is the engine speed, so the speed  $n_{s1}$  of the large sun gear and the input speed  $n_p$  of the variable pump are formulated in Equations (1) and (2).

$$n_{s1} = \begin{cases} -\frac{n_{in}}{i_3}, (HM1) \\ -\frac{n_{in}}{i_2}, (HM3) \end{cases}, \tag{1}$$

$$n_p = -\frac{n_{in}}{i_1}, \tag{2}$$

In this study, the influence of volume control speed loop volume efficiency was ignored. The relationship between quantitative motor output speed  $n_m$ , variable pump input speed  $n_p$ , and pump motor displacement ratio is shown in Equation (3). Meanwhile, the rotational speed  $n_{s2}$  of the small sun gear  $S_2$  is shown in Equation (4).

$$n_m = en_p = -\frac{en_{in}}{i_1}, \tag{3}$$

$$n_{s2} = -\frac{en_p}{i_5} = \frac{en_{in}}{i_1 i_5}, \tag{4}$$

where  $e = Q_p/Q_m = n_m/n_p$ ,  $-1 \leq e \leq 1$ .  $Q_p$  and  $Q_m$  are the instantaneous displacements of the variable displacement pump and the quantitative motor, respectively.

According to the planetary gear mechanism (PGM) speed characteristic equation [17], the input speed  $n_{s1}$  of the large sun gear  $S_1$ , the input speed  $n_{s2}$  of the small sun gear  $S_2$ , and the output speed  $n_c$  of the planetary carrier  $c$  in HM1 and HM2 gears satisfy the relationship as given in Equation (5).

$$n_c(k_1 + k_2) - k_1 n_{s2} - k_2 n_{s1} = 0, \tag{5}$$

where  $k_1 = Z_r/Z_{s1}$ ;  $k_2 = Z_r/Z_{s2}$ ;  $Z_r$  is the number of teeth of the ring gear;  $Z_{s1}$  is the number of teeth of the large sun gear; and  $Z_{s2}$  is the number of teeth of the small sun gear.

Therefore, the rotational speed  $n_c$  of planetary carrier  $c$  can be obtained in HM1 and HM3 gears, as derived in Equation (6).

$$\begin{cases} n_c = \frac{n_{in}}{k_1+k_2} \left( \frac{k_1 e}{i_1 i_5} - \frac{k_2}{i_3} \right), (HM1) \\ n_c = \frac{n_{in}}{k_1+k_2} \left( \frac{k_1 e}{i_1 i_5} - \frac{k_2}{i_2} \right), (HM3) \end{cases} \tag{6}$$

When the HMCVT output shaft is seven, the vehicle moves forward. When the output shaft is eight, the vehicle moves backwards. This is similar to the transmission method with an output shaft of seven, except for the addition of  $i_8$  and  $i_9$  to make the output speed opposite to that of shaft 7. Therefore, taking output shaft 7 as an example, the output speed of HM1 and HM3 in two forward gears can be calculated. The output speed of shaft 7  $n_o$  is shown in Equation (7). The transmission ratio  $i_g$  of HMCVT is shown in Equation (8).

$$n_o = \begin{cases} \frac{n_{in}}{(k_1+k_2)i_6 i_7} \left( \frac{k_1 e}{i_1 i_5} - \frac{k_2}{i_3} \right), (HM1) \\ \frac{n_{in}}{(k_1+k_2)i_6 i_7} \left( \frac{k_1 e}{i_1 i_5} - \frac{k_2}{i_2} \right), (HM3) \end{cases} \tag{7}$$

$$i_g = \frac{n_{in}}{n_o} = \begin{cases} \frac{(k_1 i_3 e - k_2 i_1 i_5)}{(k_1 + k_2) i_1 i_3 i_5 i_6 i_7}, (HM1) \\ \frac{(k_1 i_2 e - k_2 i_1 i_5)}{(k_1 + k_2) i_1 i_2 i_5 i_6 i_7}, (HM3) \end{cases} \tag{8}$$

### 2.1.2. Ranges HM2

In the Ravigneaux planetary gear system, the ring gear  $r$  and the small sun gear  $S_2$  are the inputs. The planet carrier  $c$  is the output. Like HM1 and HM3, the speed of the small sun gear  $S_2$  is  $n_{s2} = en_{in}/i_1 i_5$ . The speed of the ring gear  $r$  is  $n_r = -n_{in}/i_4$ . According to the PGM speed characteristic equation, the input speed  $n_r$  of the ring gear  $r$ , the input speed  $n_{s2}$  of the small sun gear  $S_2$ , and the output speed  $n_c$  of the planetary carrier  $c$  can be obtained, which satisfy the relationship shown in Equation (9).

$$n_{s2} - k_2 n_r - (1 - k_2) n_c = 0, \tag{9}$$

Therefore, the rotational speed  $n_c$  of planetary carrier  $c$  in the HM2 gear can be obtained as shown in Equation (10)

$$n_c = \frac{n_{in}}{1 - k_2} \left( \frac{e}{i_1 i_5} + \frac{k_2}{i_4} \right), \tag{10}$$

Here, taking output shaft 7 as an example, the output speed  $n_o$  of HM2 in forward gear is calculated. The output speed  $n_o$  of shaft 7 is shown in Equation (11). The transmission ratio  $i_g$  of HMCVT is shown in Equation (12).

$$n_o = \frac{n_{in}}{1 - k_2} \left( \frac{e}{i_1 i_5 i_6 i_7} + \frac{k_2}{i_4 i_6 i_7} \right), \tag{11}$$

$$i_g = \frac{n_{in}}{n_o} = \frac{(i_4 e + k_2 i_1 i_5)}{(1 - k_2) i_1 i_4 i_5 i_6 i_7}, \tag{12}$$

## 2.2. Torque Characteristic

### 2.2.1. Ranges HM1 and HM3

In the condition of ignoring power loss, which is similar to speed calculation as mentioned above, this study takes output shaft 7 as an example to calculate the HMCVT output torque  $T_o$  during the vehicle’s forward movement. The torque of  $T_o$  is shown in Equation (13).

$$T_c = \frac{T_o}{i_6 i_7}, \tag{13}$$

In the transmission process of HM1 and HM3, the input torque  $T_{in}$  is transmitted to HMCVT. The torque is divided into two parts. One part is transmitted to the variable pump of shaft 2 as  $T_p$ . The other part is transmitted to the large sun gear  $S_1$  of shaft 3 as  $T_{s1}$ . Therefore, the relationship among the input torque  $T_{in}$  and the torque of the variable pump and the large sun gear  $S_1$  is shown in Equation (14). The torque relationship between the variable pump and the quantitative motor is shown in Equation (15).

$$T_{in} = \begin{cases} -\frac{T_p}{i_1} - \frac{T_{s1}}{i_3}, & (HM1) \\ -\frac{T_p}{i_1} - \frac{T_{s1}}{i_2}, & (HM3) \end{cases}, \tag{14}$$

$$T_p = e T_m = -\frac{e T_{s2}}{i_5}, \tag{15}$$

According to Equation (5) and the PGM torque characteristic equation, it can be seen that the relationship among the input torque  $T_{s1}$  of the large sun gear  $S_1$ , the input torque  $T_{s2}$  of the small sun gear  $S_2$ , and the output torque  $T_c$  of the planetary carrier  $c$  in the HM1 and HM3 gears is shown in Equation (16).

$$M_{s1} : M_{s2} : M_c = k_2 : k_1 : -(k_1 + k_2), \tag{16}$$

According to Equation (13), the relationship between the output torque of planet carrier  $c$  and the output torque  $T_o$  of HMCVT can be determined. Equation (17) represents the input torque of the large sun gear  $S_1$  and the small sun gear  $S_2$  using the output torque  $T_c$  of the planetary carrier.

$$\begin{cases} T_{s1} = -\frac{k_2}{k_1 + k_2} T_c \\ T_{s2} = -\frac{k_1}{k_1 + k_2} T_c \end{cases}, \tag{17}$$

Thus, the relationship between the HMCVT input torque  $T_{in}$  and output torque  $T_o$  can be calculated from Equation (18) based on the above Equations (13)–(17).

$$T_{in} = \begin{cases} \frac{(k_2 i_1 i_5 - k_1 i_3 e) T_o}{i_1 i_3 i_5 i_6 i_7 (k_1 + k_2)}, & (HM1) \\ \frac{(k_2 i_1 i_5 - k_1 i_2 e) T_o}{i_1 i_2 i_5 i_6 i_7 (k_1 + k_2)}, & (HM3) \end{cases}, \quad (18)$$

Finally, the ratio  $\mu$  between the output torque of HMCVT and the input torque of the engine in the HM1 and HM3 gears is expressed in Equation (19).

$$\mu = \frac{T_o}{T_{in}} = \begin{cases} \frac{i_1 i_3 i_5 i_6 i_7 (k_1 + k_2)}{(k_2 i_1 i_5 - k_1 i_3 e)}, & (HM1) \\ \frac{i_1 i_2 i_5 i_6 i_7 (k_1 + k_2)}{(k_2 i_1 i_5 - k_1 i_2 e)}, & (HM3) \end{cases}, \quad (19)$$

### 2.2.2. Ranges HM2

In the HM2 gear, the HMCVT output torque  $T_o$  is also represented by Equation (13). In the transmission process of HM2, the input torque  $T_{in}$  is divided into two parts. One part is transmitted to the variable pump of shaft 2 as  $T_p$  and the other part is transmitted to the ring gear r as  $T_r$ . Therefore, the relationship among the input torque  $T_{in}$  and the torque of the variable displacement pump and the annular ring gear r is shown in Equation (20).

$$T_{in} = -\frac{T_p}{i_1} - \frac{T_r}{i_4}, \quad (20)$$

Similarly to the torque calculation of HM1 and HM3, it can be seen that in the HM2 gear, the relationship among the input torque  $T_r$  of the ring gear r, the input torque  $T_{s2}$  of the small sun gear  $S_2$ , and the output torque  $T_c$  of the planetary carrier c is shown in Equation (21).

$$M_r : M_{s2} : M_c = -k_2 : 1 : -(1 - k_2), \quad (21)$$

In Equation (22), the output torque  $T_c$  of the planetary carrier is used to represent the input torque between the ring gear r and the small sun gear  $S_2$ .

$$\begin{cases} T_r = \frac{k_2}{1 - k_2} T_c \\ T_{s2} = \frac{1}{k_2 - 1} T_c \end{cases}, \quad (22)$$

Thus, the relationship between the HMCVT input torque  $T_{in}$  and output torque  $T_o$  can be calculated according to Equations (20)–(22), as shown in Equation (23).

$$T_{in} = \frac{(i_4 e + k_2 i_6 i_7) T_o}{i_1 i_4 i_5 i_6 i_7 (k_2 - 1)}, \quad (23)$$

Finally, the ratio  $\mu$  between the output torque of HMCVT and the input torque of the engine in the HM2 gear is derived from Equation (24).

$$\mu = \frac{T_o}{T_{in}} = \frac{i_1 i_4 i_5 i_6 i_7 (k_2 - 1)}{(i_4 e + k_2 i_6 i_7)}, \quad (24)$$

### 2.3. Transmission Efficiency Analysis

In this study, the Крейнс method [18], as shown in Equation (25), is introduced to calculate the transmission efficiency of HMCVT.

$$\eta = -\tilde{\mu} / i_g = -\frac{T_o / T_e}{n_e / n_o}, \quad (25)$$

where  $\tilde{\mu}$  is the ratio of output torque to input torque; and  $i_g$  is the HMCVT ratio.

The torque considering power loss for HMCVT in each working range is shown in Tables 1 and 2. Among them, the transmission efficiency calculation process of HM1 and HM3 is listed in Table 1 and the transmission efficiency calculation process of HM2 is listed in Table 2. In Tables 1 and 2,  $\eta_{1-7}$  is the transmission efficiency of the  $i_1-i_7$  gear pair.  $\eta_H$  is the transmission efficiency of the hydraulic system.  $\eta_{rs1}$  and  $\eta_{rs2}$  are the transmission efficiencies from the ring gear r to the large sun gear  $S_1$  and from the ring gear r to the small sun gear  $S_2$ , respectively.

**Table 1.** Equation of efficiency calculation for HM1 and HM3 ranges.

Elements	HM1 $e > 0$	HM3 $e > 0$	HM1 $e < 0$	HM3 $e < 0$
Engine	$T_e = -\frac{T_p \eta_1}{i_1} - \frac{T_{s1}}{i_3 \eta_3}$	$T_e = -\frac{T_p \eta_1}{i_1} - \frac{T_{s1}}{i_2 \eta_2}$	$T_e = -\frac{T_p}{i_1 \eta_1} - \frac{T_{s1}}{i_3 \eta_3}$	$T_e = -\frac{T_p}{i_1 \eta_1} - \frac{T_{s1}}{i_2 \eta_2}$
Pump	$T_p = e T_m \eta_H$		$T_p = e T_m / \eta_H$	
Motor	$T_m = -T_{s2} \eta_5 / i_5$		$T_m = -T_{s2} / \eta_5 i_5$	
PGM	$T_{s1} + T_{s2} + T_c = 0$			
Intermediate shaft	$T_c = T_o / i_6 i_7 \eta_6 \eta_7$			
Sun gear 1	$T_{s1} = -k_2 \eta_{rs2} T_c / (k_1 \eta_{rs1} + k_2 \eta_{rs2})$			
Sun gear 2	$T_{s2} = -k_1 \eta_{rs1} T_c / (k_1 \eta_{rs1} + k_2 \eta_{rs2})$			
$\tilde{\mu}$	$T_o / T_e$ (Consider efficiency loss at this point)			
$n_{in} / n_o$	$\frac{(k_1 + k_2) i_1 i_3 i_5 i_6 i_7}{(k_1 i_3 e - k_2 i_1 i_5)}$	$\frac{(k_1 + k_2) i_1 i_2 i_5 i_6 i_7}{(k_1 i_2 e - k_2 i_1 i_5)}$	$\frac{(k_1 + k_2) i_1 i_3 i_5 i_6 i_7}{(k_1 i_3 e - k_2 i_1 i_5)}$	$\frac{(k_1 + k_2) i_1 i_2 i_5 i_6 i_7}{(k_1 i_2 e - k_2 i_1 i_5)}$

**Table 2.** Equation of efficiency calculation for HM2 ranges.

Elements	HM2 $e > 0$	HM2 $e < 0$
Engine	$T_e = -\frac{T_p}{i_1 \eta_1} - \frac{T_r}{i_4 \eta_4}$	$T_e = -\frac{T_p \eta_1}{i_1} - \frac{T_r}{i_4 \eta_4}$
Pump	$T_p = e T_m / \eta_H$	
Motor	$T_m = -T_{s2} / i_5 \eta_5$	
PGM	$T_r + T_{s2} + T_c = 0$	
Intermediate shaft	$T_c = T_o / i_6 i_7 \eta_6 \eta_7$	
Ring gear	$T_r = k_2 \eta_{rs2} T_c / (1 - k_2 \eta_{rs2})$	
Sun gear 2	$T_{s2} = T_c / (k_2 \eta_{rs2} - 1)$	
$\tilde{\mu}$	$T_o / T_e$ (Consider efficiency loss at this point)	
$n_{in} / n_o$	$\frac{(1 - k_2) i_1 i_4 i_5 i_6 i_7}{(i_4 e + k_2 i_1 i_5)}$	

In the HMCVT gearbox, the output torque  $T_e$  of the engine is the input torque  $T_{in}$  of the HMCVT. The output speed  $n_e$  of the engine is the input speed  $n_{in}$  of the HMCVT. Taking the calculation of transmission efficiency in HM1 with  $e$  (displacement ratio) greater than 0 as an example explains the Крейнес method. In Table 1,  $T_{in}$  can be represented by  $T_p$  and  $T_{s1}$ .  $T_p$  can be represented by  $T_m$ .  $T_m$  can be represented by  $T_{s2}$ .  $T_{s1}$  and  $T_{s2}$  can be represented by  $T_c$  according to the PGM equation. According to Equation (13), the relationship between  $T_c$  and  $T_o$  can be known.

According to the torque and speed transmission relationship in HMCVT,  $\tilde{\mu}$  and  $i_g$  in Equation (25) can be obtained. The transmission efficiency of HMCVT can be calculated using Equation (25).

Finally, the transmission efficiency within different displacement ratio ranges of the HM1/HM2/HM3 gears can be obtained numerically, as calculated in Equation (26) below.

$$\eta_{HM1} = \begin{cases} \frac{(k_1\eta_{rs1}+k_2\eta_{rs2})(k_2i_1i_5-k_1i_3e)\eta_3\eta_6\eta_7}{(k_1+k_2)(k_2i_1i_5\eta_{rs2}-k_1i_3e\eta_1\eta_3\eta_5\eta_{rs1}\eta_H)}, (e > 0) \\ \frac{(k_1\eta_{rs1}+k_2\eta_{rs2})(k_2i_1i_5-k_1i_3e)\eta_1\eta_3\eta_5\eta_6\eta_7\eta_H}{(k_1+k_2)(k_2i_1i_5\eta_1\eta_5\eta_{rs2}\eta_H-k_1i_3e\eta_3\eta_{rs1})}, (e \leq 0) \end{cases}$$

$$\eta_{HM2} = \begin{cases} \frac{(k_2\eta_{rs2}-1)(i_4e+k_2i_1i_5)\eta_1\eta_4\eta_5\eta_6\eta_7\eta_H}{(k_2-1)(i_4e\eta_4+k_2i_1i_5\eta_1\eta_5\eta_{rs2}\eta_H)}, (e > 0) \\ \frac{(k_2\eta_{rs2}-1)(i_4e+k_2i_1i_5)\eta_4\eta_6\eta_7}{(k_2-1)(i_4e\eta_1\eta_4\eta_5\eta_H+k_2i_1i_5\eta_{rs2})}, (e \leq 0) \end{cases}$$

$$\eta_{HM3} = \begin{cases} \frac{(k_1\eta_{rs1}+k_2\eta_{rs2})(k_2i_1i_5-k_1i_2e)\eta_2\eta_6\eta_7}{(k_1+k_2)(k_2i_1i_5\eta_{rs2}-k_1i_2e\eta_1\eta_2\eta_5\eta_{rs1}\eta_H)}, (e > 0) \\ \frac{(k_1\eta_{rs1}+k_2\eta_{rs2})(k_2i_1i_5-k_1i_2e)\eta_1\eta_2\eta_5\eta_6\eta_7\eta_H}{(k_1+k_2)(k_2i_1i_5\eta_1\eta_5\eta_{rs2}\eta_H-k_1i_2e\eta_2\eta_{rs1})}, (e \leq 0) \end{cases} \quad (26)$$

### 3. HMCVT Optimization for Coupling Comprehensive Transmission Efficiency and Shifting Smoothness Across All Gears

#### 3.1. Determination of HMCVT Parameters

The engine speed matched with HMCVT is 2200 r/min. The driving speed and gear information of the tractor in different gears are tabulated in Table 3. The maximum speed is 50 km/h. The main reduction ratio  $i_{z1}$  is 1.29 and the driving wheel radius is 0.858 m.

**Table 3.** Displacement ratio, vehicle speed, clutch engagement, and information of tractor in different gears.

	e	Speed (km/h)	C1	C2	C3
HM1	(−0.92, 0.82)	0–16	✓	/	/
HM2	(−0.92, 0.96)	16–32	/	✓	/
HM3	(−1, 0.96)	32–50	/	/	✓

Note: e is displacement ratio of hydraulic pump to hydraulic motor. C1 is clutch 1, C2 is clutch 2, C3 is clutch 3. Check mark is used to indicate whether C1, C2, and C3 corresponding to each speed range are engaged.

When HMCVT switches between adjacent gears, the displacement ratio and transmission ratio at the change point must meet the conditions shown in Equation (27).

$$\begin{cases} i_{g\_HM1}(0.82) = \infty, \\ i_{g\_HM1}(-0.92) = i_{g\_HM2}(-0.92), \\ i_{g\_HM2}(0.96) = i_{g\_HM3}(0.96), \\ i_{g\_HM3}(-1) = i_{min}, \end{cases} \quad (27)$$

According to the vehicle information in Table 3 and Equation (27), the relationship among the HMCVT gear pair transmission ratio,  $k_1$  and  $k_2$  can be obtained, as shown in Equation (28).

$$\begin{cases} 0.82k_1i_3 = k_2i_1i_5 \\ \frac{0.92k_1i_3+k_2i_1i_5}{i_3(k_1+k_2)} = \frac{k_2i_1i_5-0.92i_4}{i_4(1-k_2)} \\ \frac{0.96i_4+k_2i_1i_5}{i_4(1-k_2)} = \frac{0.96k_1i_2-k_2i_1i_5}{i_2(k_1+k_2)} \\ \frac{k_1i_2+k_2i_1i_5}{(k_1+k_2)i_1i_2i_5i_6i_7} = 0.091 \end{cases} \quad (28)$$

There are a total of nine parameters to be solved for HMCVT in Equation (28), with only four equations. Therefore, when solving the HMCVT parameters, it is necessary to firstly assign values to five parameters and then calculate the remaining four parameters.

Meanwhile, during the calculation process, it should be noted that the transmission ratio  $i_{g_{HM1toHM2}}$  at the transition point between the HM1 and HM2 gears is smaller than the transmission ratio  $i_{g_{HM2toHM3}}$  at the transition point between the HM2 and HM3 gears.

Therefore, the planetary gear mechanism (PGM) structure parameters  $k_1$  is set to 3.5,  $i_1$  is 1.5,  $i_3$  is 4,  $i_6$  is 3, and  $i_7$  is 3.5. The remaining four transmission ratio parameters can be calculated using Equation (28). The remaining parameters of HMCVT are calculated as follows:  $k_2$  is 3.98,  $i_2$  is 0.74,  $i_4$  is 3.09, and  $i_5$  is 1.58. All parameters are recorded in Table 4. In Section 4 an HMCVT model was established based on nine transmission ratio parameters, which can determine its variable speed transmission law based on the input transmission ratio parameters. By inputting the nine transmission ratios into the Simulink model built in Section 4, the output speed curve and transmission efficiency can be obtained.

**Table 4.** One set of calculated transmission ratio values.

Transmission Parameters	$k_1$	$k_2$	$i_1$	$i_2$	$i_3$	$i_4$	$i_5$	$i_6$	$i_7$
value	3.5	3.98	1.5	0.74	4	3.09	1.58	3	3.5

### 3.2. Structural Optimization of HMCVT Using Improved NSGA-II

By using Equations (27) and (28), the HMCVT structural parameters that conform to the shifting pattern in Table 3 can be calculated. In this section, considerations for HMCVT efficiency and shifting smoothness are included in the calculation of transmission parameters [19]. Redesign HMCVT parameters using an improved NSGA-II genetic algorithm. The optimized genetic algorithm can improve overall transmission efficiency and shifting smoothness while meeting the design requirements of the gearbox. At the same time, the algorithm introduces the concept of simulated annealing in the calculation of mutation operators to avoid being stuck in local optima and increase the algorithm’s fine-tuning ability.

#### 3.2.1. Objective Function and Constraint Condition

The transmission efficiency and the effective connection between adjacent gear speed points are related to the PGM structure parameters  $k$  and the gear pair tooth ratio. The design of gear parameters will have a direct impact. The objective function  $\min f(X1)$  includes the difference in transmission ratios between adjacent gears at all gear transition points, as well as the difference between the initial/end points of the continuously variable transmission and the theoretical data, as shown in Equation (29). The objective function  $\min f(X2)$  includes the comprehensive transmission efficiency of HM1-HM3 working sections. The transmission efficiency of different points on each working section is calculated at intervals of 0.1 to obtain comprehensive transmission efficiency, as shown in Equation (30). Because it calculates the maximum comprehensive efficiency, but seeks the minimum value during the optimization process, Equation (30) is therefore transformed using the method shown in Equation (31).

$$\min f(X1) = |1/i_{g_{HM1}(0.82)}| + |i_{g_{HM1}(-0.92)} - i_{g_{HM2}(-0.92)}| + |i_{g_{HM2}(0.96)} - i_{g_{HM3}(0.96)}| + |i_{max} - i_{g_{HM3}(-1)}|, \quad (29)$$

$$\min f(X2) = 10 \times \left\{ \begin{array}{l} \sum_{e=-0.92,0.1}^0 \eta_{HM1}(e)/10 + \sum_{e=0,0.1}^{0.82} \eta_{HM1}(e)/9 + \\ \sum_{e=-0.92,0.1}^0 \eta_{HM2}(e)/10 + \sum_{e=0,0.1}^{0.96} \eta_{HM2}(e)/10 + \\ \sum_{e=-1,0.1}^0 \eta_{HM3}(e)/11 + \sum_{e=0,0.1}^{0.96} \eta_{HM3}(e)/10 \end{array} \right\} /6, \quad (30)$$

$$\min f(X2) = 1/\min f(X2), \quad (31)$$

The decision variable is a related parameter that can directly affect the value of the objective function. According to Equations (29)–(31), the decision variable is the transmission ratio  $i$  of each gear pair and the parameters  $k_1$  and  $k_2$  of the planetary gear set, that is

$$X = [k_1, k_2, i_1, i_2, i_3, i_4, i_6], \quad (32)$$

The speed range of the tractor is 0–50 km/h, the speed range of the HM1 working section is 0– $y_1$  km/h, the speed range of the HM2 working section is  $y_1$ – $y_2$  km/h, and the speed range of the HM3 working section is  $y_2$ –50 km/h. The driving speed of the tractor can be expressed as Equation (33).

$$v = 0.377 \frac{n_{in} r}{i_g i_{z1}} = \frac{551.65}{i_g}, \quad (33)$$

The constraint conditions for the transmission ratio in three gears are shown in Equation (34). The constraints between the shifting points of multiple working stages satisfy Equation (27).

$$\left\{ \begin{array}{l} 0 \leq \frac{551.65}{i_{g\_HM1}} \leq y_1 \\ y_1 \leq \frac{551.65}{i_{g\_HM2}} \leq y_2 \\ y_2 \leq \frac{551.65}{i_{g\_HM3}} \leq 50 \end{array} \right. , \quad (34)$$

### 3.2.2. Optimization of HMCVT Configuration via NSGA-II

The NSGA-II genetic algorithm is an adaptive random search algorithm that simulates the natural process of survival of the fittest and it is widely used to solve nonlinear, multi-objective optimization problems [20]. The analysis of HMCVT parameters is quite complex. In order to improve the applicability and accuracy of genetic algorithms, the traditional NSGA-II genetic algorithm is improved by introducing the concept of simulated annealing into the mutation operator calculation of the NSGA-II genetic algorithm. As the population continues to evolve, individuals within the population gradually tend to stabilize and the probability of compilation also decreases. Therefore, a mutation operator incorporating simulated annealing is used to enhance the stability of the genetic algorithm. The improved mutation operator is shown in Equation (35).

$$pm = pm_0 \times (0.9)^{n \times r}, \quad (35)$$

where  $pm_0$  is the original mutation operator;  $n$  is the current generation of the population and the maximum generation of the population is set to  $n_{ge}$ ; and  $r$  is the constant of the simulated annealing algorithm, taken as 0.95 here.

At the same time, the non-uniform mutation approach is introduced to establish a relationship between the role of mutation operators and evolutionary algebra, in order to ensure that the stability of the genetic algorithms is enhanced while also improving their

local search capabilities. Assuming that in the  $n$ th generation population, individual  $m$  ( $m_1, m_2, m_3, m_4, m_5, m_6, m_7$ ) undergoes mutation, a uniform random selection method is used to mutate one of the gene values  $m_j$ . The specific way of mutation is shown in Equations (36) and (37). During the mutation process,  $rand_2$  is used to determine the calculation method of  $m_j$  and  $k$ , enhancing the randomness of the mutation process. After mutation, the gene of the new individual  $m$  becomes  $(m_1, m_2, \dots, m_j, \dots, m_7)$ .

$$m_j = \begin{cases} m_j + k \times (1 - rand_1^{(1-n/n_{ge})^b}), & rand_2 \geq 0.5 \\ m_j - k \times (1 - rand_1^{(1-n/n_{ge})^b}), & else \end{cases}, \tag{36}$$

$$k = \begin{cases} bound(j, 2) - m_j, & rand_2 \geq 0.5 \\ m_j - bound(j, 1), & else \end{cases} \tag{37}$$

where  $rand_1$  and  $rand_2$  are both random numbers within the range of 0–1;  $b$  is the uniformity parameter, generally ranging from 2 to 5; and  $bound(j, 1)$  and  $bound(j, 2)$  are the lower and upper limits of the value of the  $j$ th gene, respectively.

In this study, the NSGA-II genetic algorithm introduces the concept of simulated annealing and uniform mutation characteristics, as shown in Figure 2. Firstly, in the initial stage of optimization, set the initial population size, initial crossover probability, genetic probability, and maximum number of iterations. Secondly, initialize the population based on the optimization objective function mentioned above. Thirdly, non-dominated sorting of the population is performed based on the calculated fitness. Fourth, select outstanding individuals for crossover and mutation. Each generation of the population uses Equation (35) to calculate the mutation operator, and Equations 36 and 37 to calculate the mutated individuals.

By comparing the optimization process of HMCVT design parameters before and after algorithm improvement, the results shown in Figure 3 can be obtained. The improved genetic algorithm has better optimization performance within the same evolutionary generation. In the 10th generation, the original genetic algorithm’s  $min f(X1)$  (HMCVT shift loss) can be reduced to a minimum of 0.071; the improved genetic algorithm’s  $min f(X1)$  can be reduced to 0.025, a decrease of 65.6%; and  $min f(X2)$  (HMCVT loss) can be reduced from 0.27 to 0.12, a decrease of 56.2%. In the 20th generation, the original genetic algorithm’s  $min f(X1)$  can be reduced to a minimum of 0.065, while the improved genetic algorithm’s  $min f(X1)$  can be reduced to 0.015, a decrease of 76.3%;  $min f(X2)$  has decreased from 0.20 to 0.11, a decrease of 48.2%. In the 50th generation, the original genetic algorithm’s  $min f(X1)$  results were concentrated between 0.06 and 0.11, while the improved genetic algorithm’s  $min f(X1)$  results were concentrated between 0.01 and 0.04;  $min f(X2)$  decreased from the original (0.2, 0.3) to (0.1, 0.225). Overall, the introduction of simulated annealing and non-uniform mutation characteristics in the NSGA-II genetic algorithm has improved the optimization performance of the algorithm.

By adopting a weighted approach to select the optimal point on the Pareto front of the 50th generation optimization algorithm, the weights of  $min f(X1)$  and  $min f(X2)$  are both 0.5. The HMCVT optimized transmission parameters are ultimately selected as shown in Table 5.

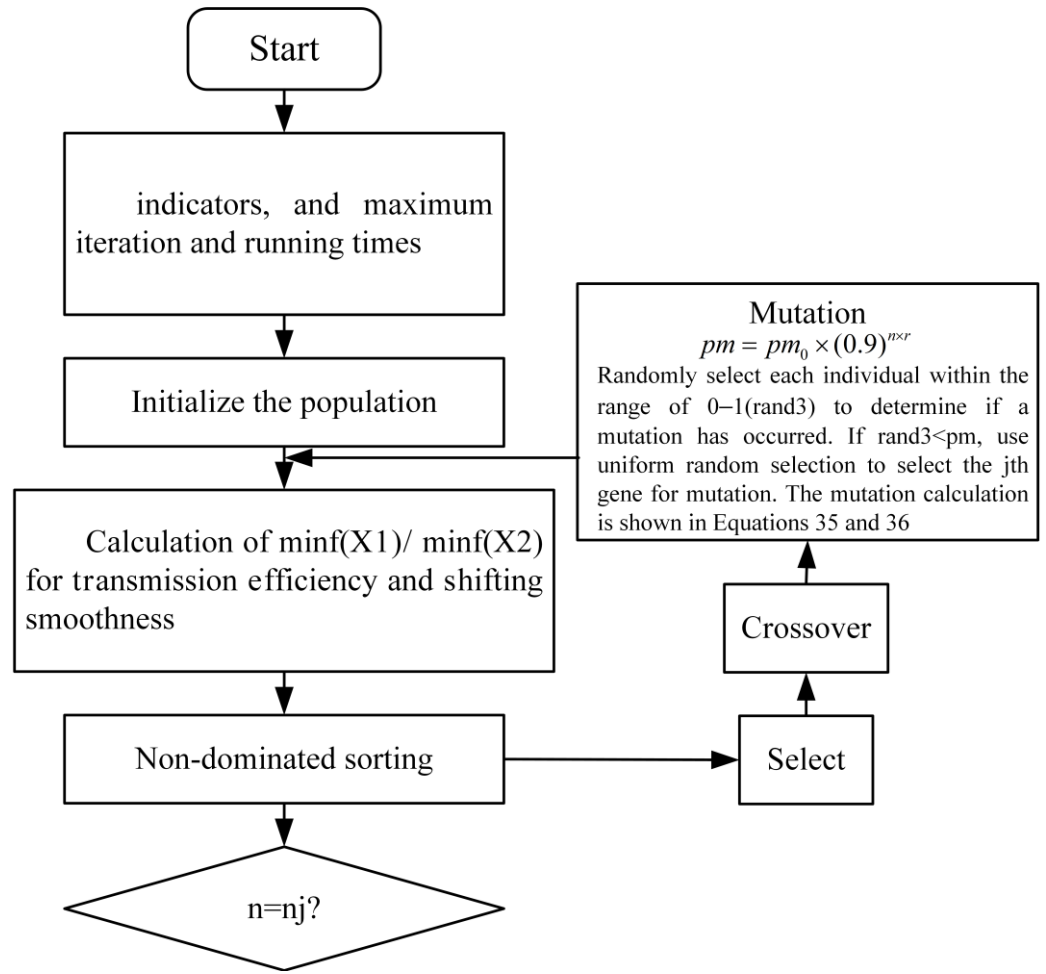


Figure 2. Optimization design process of HMCVT for improved NSGA-II.

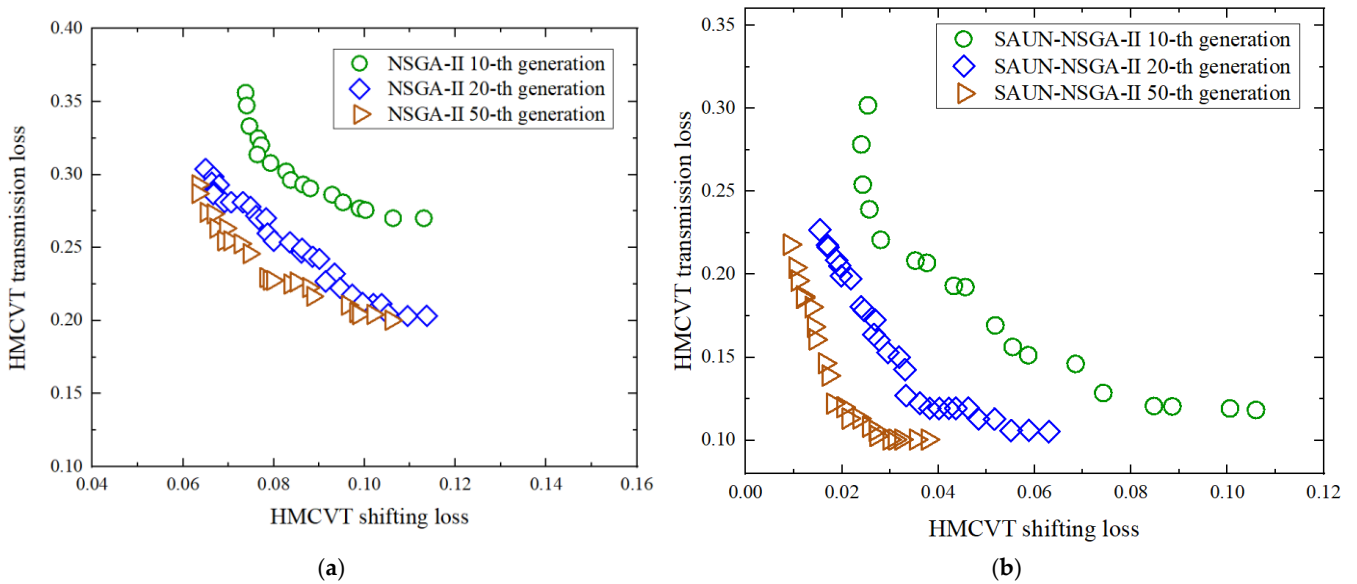


Figure 3. Multi-objective optimization results of (a) NSGA-II and (b) improved NSGA-II.

**Table 5.** NSGA-II and improved NSGA-II transmission ratio values.

Transmission Parameters	$k1$	$k2$	$i1$	$i2$	$i3$	$i4$	$i5$	$i6$	$i7$
Value1 (NSGA-II)	4.4	7.8	5.1	2.6	11.2	7.7	1	3.5	1
Value2 (improved NSGA-II)	4.8	6.1	7	2.5	11	9	1	3.1	1

### 4. HMCVT Optimization Verification and Results

This section validates the transmission analysis in Section 2 and the transmission efficiency optimization in Section 3. A gearbox transmission efficiency simulation platform was built using Simulink in the MATLAB R2022b(64-bit) Section 4.2 showed that the structural optimization algorithm can play a certain role in optimizing the transmission efficiency of high-power tractors.

#### 4.1. The Composition of Each Part of the HMCVT Model

From Figure 4, it can be seen that the Simulink model of HMCVT consists of five parts, which include the target speed information, engine, HMCVT speed controller, HMCVT, and transmission efficiency analysis module. The engine provides input speed  $n_{in}$  and input torque  $T_{in}$  for HMCVT. The speed message transmits the target output speed of HMCVT to the transmission controller. The controller modulates the change in displacement ratio  $e$  and gear switching of the hydraulic module inside the transmission based on the output speed  $n_{out}$  and target output speed  $aim\_n_{out}$  of HMCVT. HMCVT can perform corresponding actions based on the  $e$  and clutch engagement/disengagement signals provided by the transmission controller and calculate the output speed and torque of HMCVT [21].

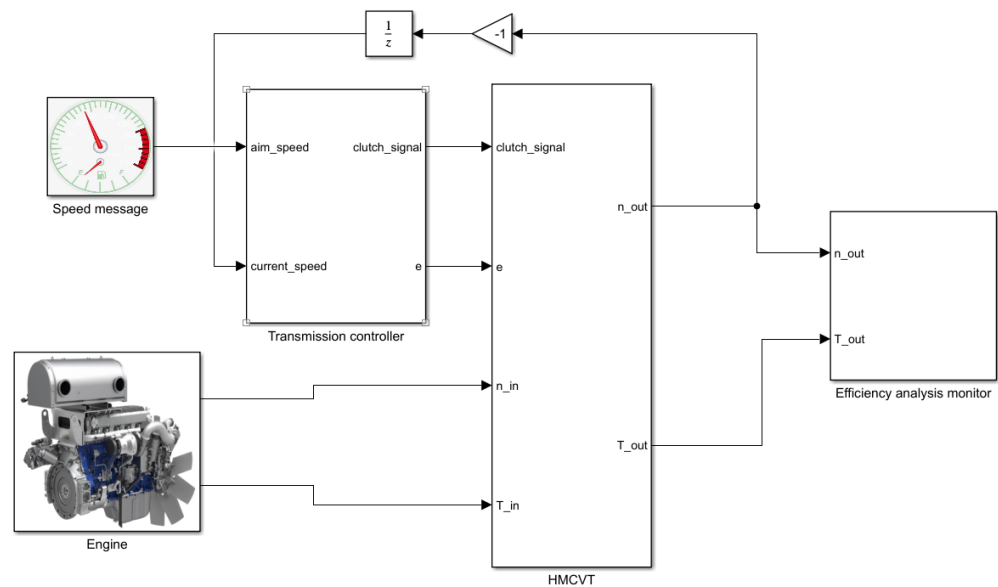


**Figure 4.** HMCVT simulation model.

#### 4.2. HMCVT Speed Controller Verification

The transmission controller is shown in Figure 5. Figure 5 is the internal structure of the transmission controller, which adjusted the value of  $u$  input to displacement ratio and gear controller through PID controller. It shows the control logic of the HMCVT gear to the displacement ratio created through Stateflow in Simulink. The shift\_state module can determine the clutch signal for switching between three gears. The pump\_state

module below can calculate the change in the displacement ratio. The final output signal is transmitted to HMCVT in Figure 4.

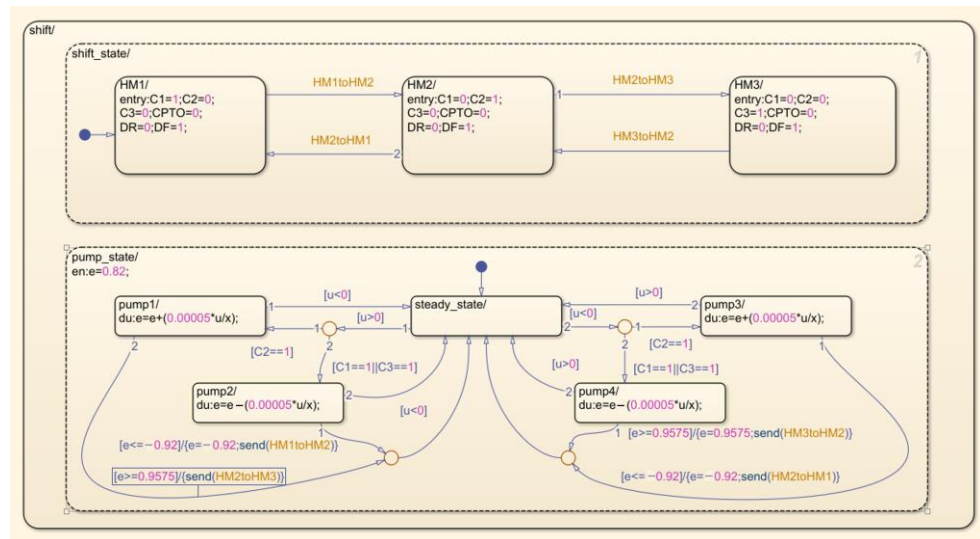


Figure 5. Transmission controller.

The simulation time for model testing is set to 300 s, and the simulation step size is 0.1 s. The change in the displacement of the pump motor module is shown in Figure 6.

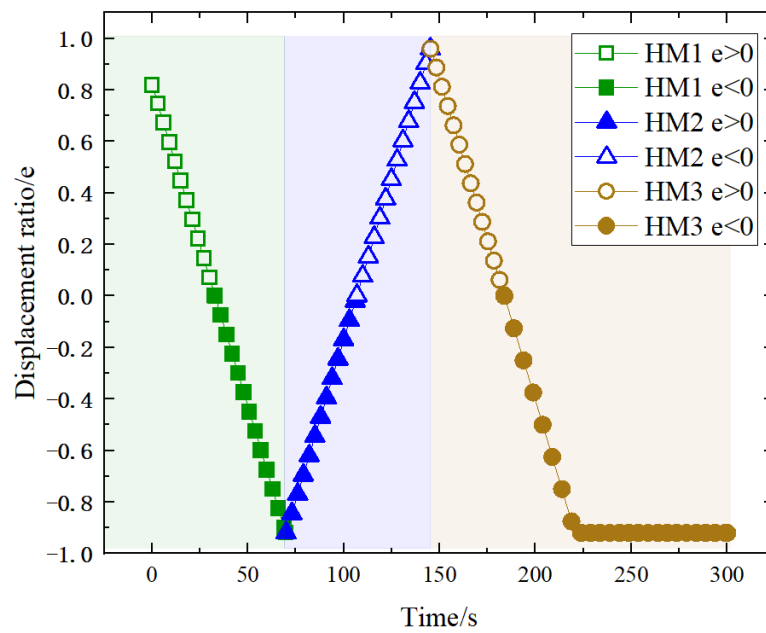
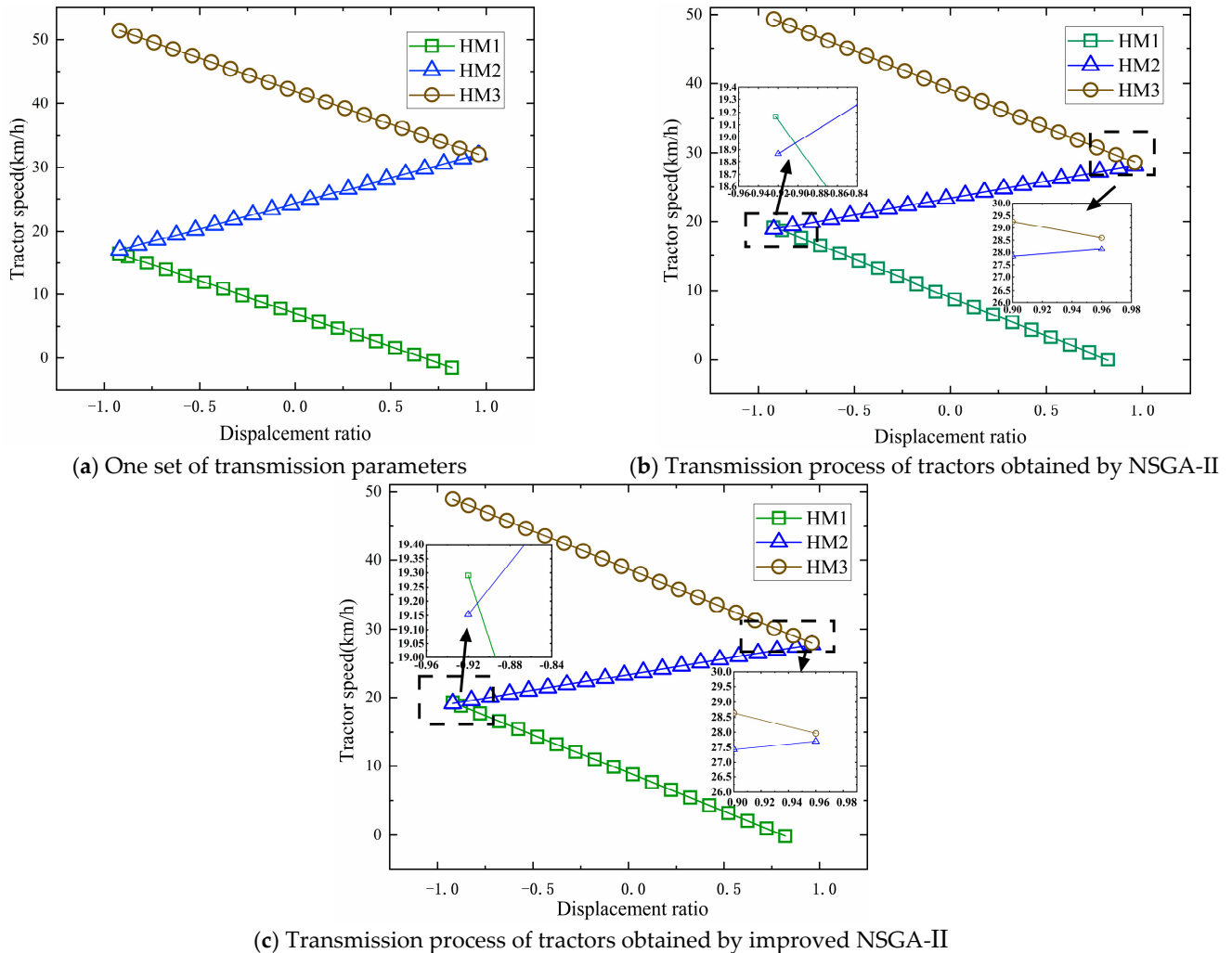


Figure 6. Pump motor displacement variation.

#### 4.3. Model Simulation Results

By inputting the HMCVT parameters calculated in Section 3.1 and the optimized parameters in Section 3.2 into the HMCVT Simulink model for simulation, the vehicle speed variation process shown in Figure 7 can be obtained. It can be seen that compared to the original speed range in Figure 7a, the optimization of the HMCVT structure considers shifting smoothness and comprehensive transmission efficiency, and the working range of HM2 is more concentrated in the range of 20–30 km/h. It can be seen that the optimization algorithm can achieve smooth shifting and optimal comprehensive transmission efficiency

during the dynamic change in shifting points. Meanwhile, in the 50th generation population, compared to NSGA-II, the improved NSGA-II reduced the error of HM1-HM2 by changing short joints from 0.31 km/h to 0.15 km/h, and reduced the error of HM2-HM3 by changing segment connection points from 0.46 km/h to 0.26 km/h, making the segment change process smoother.



**Figure 7.** The curve of the tractor speed.

Meanwhile, Figure 8 shows the transmission efficiency of the three sets of transmission parameters obtained in different ways during the simulation process. The transmission configuration using the NSGA-II genetic algorithm and the improved genetic algorithm can achieve the best comprehensive transmission efficiency and smooth shifting within a certain range of transmission ratios. From Figure 8b,c, it can be seen that the ordinary NSGA-II optimization algorithm and the improved NSGA-II optimization algorithm adjust the second speed range of the original design parameters from 16 to 32 km/h to 19–28 km/h. The improved genetic algorithm has slightly improved compared to NSGA-II in the HM2 working stage, with an efficiency increase of 0.67% at the maximum transmission efficiency point. In summary, optimizing the transmission structure parameters of HMCVT through the improved NSGA-II genetic algorithm can more effectively improve the overall transmission efficiency of HMCVT and promote smooth gear shifting.

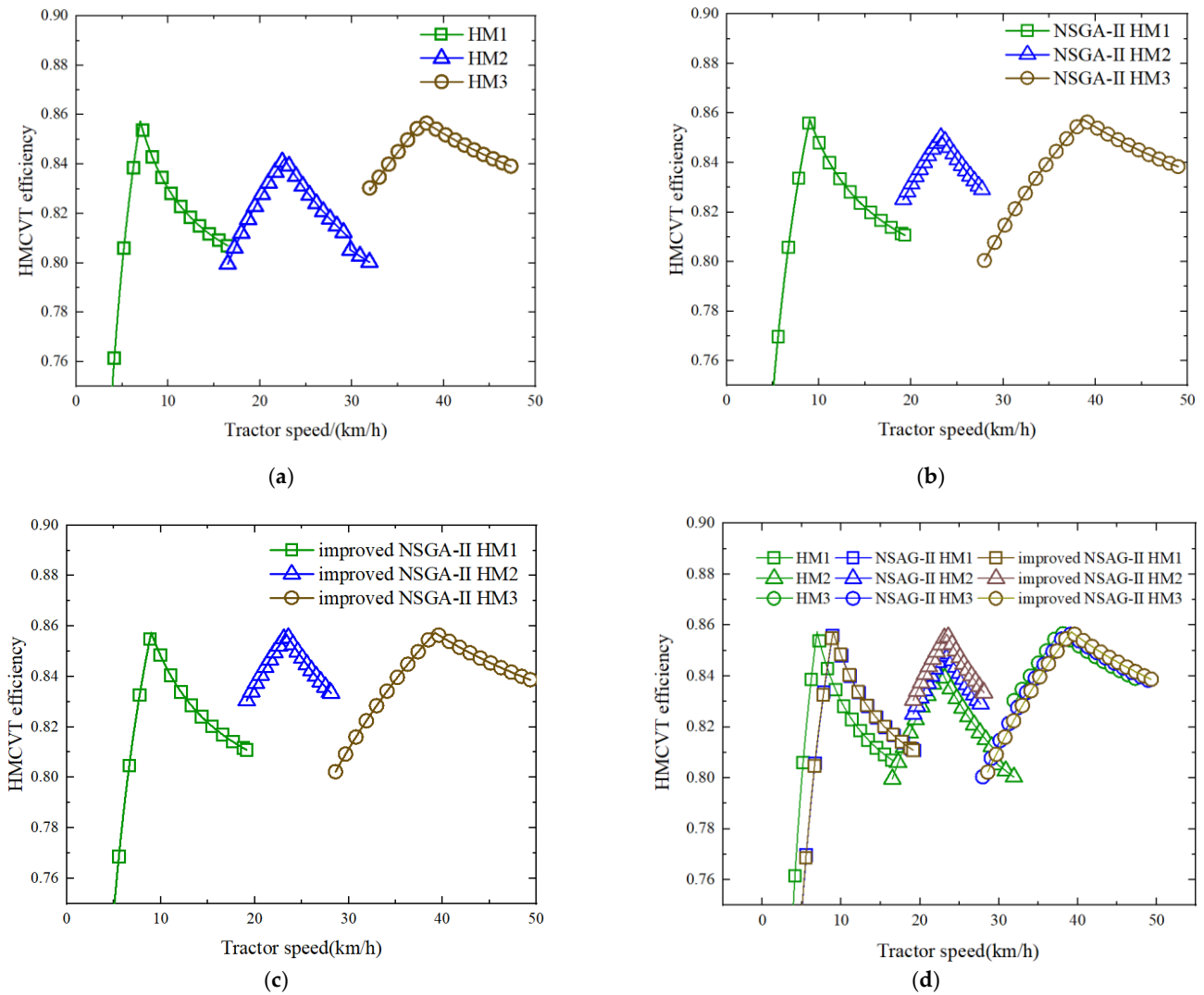


**Figure 8.** Curve of HMCVT efficiency. (a) HMCVT efficiency based on calculated transmission ratio. (b) HMCVT efficiency obtained by optimizing transmission ratio using NSGA-II. (c) HMCVT efficiency obtained by optimizing transmission ratio using improved NSGA-II. (d) HMCVT efficiency of transmission ratios obtained through three different methods: ordinary calculation, NSGA-II, and improved NSGA-II.

### 5. Discussion

To verify the effectiveness of the method, this HMCVT was tested in a transmission efficiency simulation platform. The transmission efficiency results of the three working stages are roughly equal to the true values, and the proposed Крейнес calculation method can effectively evaluate the transmission efficiency of this new HMCVT. At the same time, based on the distribution characteristics of transmission efficiency in the working section, the changing trend of transmission efficiency in the HM1 working section can be seen. It can be seen that in the part where the displacement ratio is greater than 0, the rate of increase in transmission efficiency slows down, while in the HM1 working section where the displacement ratio is less than 0, the rate of decrease in transmission efficiency slows down. This phenomenon also exists in the HM2 and HM3 working stages. To minimize the loss of transmission efficiency as much as possible, it is possible to consider how to improve the phenomenon of slowing down the rate of increase in transmission efficiency, while also optimizing the ability to slow down the rate of decrease in transmission efficiency.

Meanwhile, based on the continuous variation in the displacement ratio of HMCVT and the engagement and disengagement of the clutch, it can be concluded that the controller of HMCVT has achieved effective control. By issuing the desired displacement ratio and clutch engagement/disengagement signal, continuous variation in HMCVT output speed was achieved.

By comparing the corresponding transmission efficiency results of HMCVT parameters obtained by three different methods, it can be seen that the optimized NSGA-II algorithm achieves dynamic optimization of transmission parameters through different combinations of transmission ratios and shift points. After optimization, the transmission efficiency of the three working sections was significantly improved. At the same time, the range of the entire HM2 working section is shortened, indicating that the appropriate shortening of the HM2 working section of this HMCVT has a certain effect on improving the overall transmission efficiency.

## 6. Conclusions

This paper proposes a new transmission scheme for HMCVT. The variable speed structure is composed of a Ravigneaux planetary gear set and a pump motor module connected in parallel. According to the displacement ratio of the control clutch and pump motor module, HMCVT achieves a continuously variable transmission of a tractor within 0–50 km/h.

According to the design requirements, a new HMCVT configuration would be derived via the intelligent optimization algorithm. The goal is to achieve optimal shifting smoothness and comprehensive transmission efficiency with the constraint of a continuously variable transmission within 0–50 km/h. Improved NSGA-II realizes dynamic optimization of HMCVT parameters with unrestricted gear shifting speed. Introducing the concept of simulated annealing and uniform mutation into the mutation process of the NSGA-II algorithm not only enhances the stability of genetic algorithm but also improves its local search capability. Under the same algebraic population conditions, the improved genetic algorithm has abilities on modulating transmission configurations with better shifting smoothness and higher overall transmission efficiency.

**Author Contributions:** Conceptualization, W.Y. and F.Z.; methodology, Z.M.; software, Z.M.; validation, Z.M.; formal analysis, H.L. (Hongyu Liu) and H.L. (He Li); investigation, Q.W.; resources, Z.L.; data curation, Y.C.; writing—original draft preparation, Z.M.; writing—review and editing, W.Y., F.Z. and Z.M.; visualization, D.S.; supervision, J.Z.; project administration, L.Z.; funding acquisition, W.Y. and F.Z. All authors have read and agreed to the published version of the manuscript.

**Funding:** This research was funded by National Key R&D Program of China (No. 2021YFD2000302) and the Shandong Provincial Natural Science Foundation (No. 2022HWYQ-061).

**Data Availability Statement:** No new data were created or analyzed in this study. Data sharing is not applicable to this article.

**Acknowledgments:** The authors greatly acknowledge technical support from AVL List Technical Center (Shanghai) Co., Ltd.

**Conflicts of Interest:** Author Zhengyu Li, Deming Sun, Yanbin Cai and Jiwei Zhang was employed by the company WeiChai Lovol Intelligent Agricultural Technology Co. Author Long Zhou was employed by the company AVL List Technical Center (Shanghai) Co. The remaining authors declare that the research was conducted in the absence of any commercial or financial relationships that could be construed as a potential conflict of interest.

## References

1. Liu, Z.; Zhang, G.; Chu, G.; Niu, H.; Zhang, Y.; Yang, F. Design matching and dynamic performance test for an HST-based drive system of a hillside crawler tractor. *Agriculture* **2021**, *11*, 466. [\[CrossRef\]](#)
2. Gupta, B.; Madan, G.; Md, A.Q. A smart agriculture framework for IoT based plant decay detection using smart croft algorithm. *Mater. Today Proc.* **2022**, *62*, 4758–4763. [\[CrossRef\]](#)
3. Cheng, Z.; Lu, Z. Research on HMCVT parameter design optimization based on the service characteristics of agricultural machinery in the whole life cycle. *Machines* **2023**, *11*, 596. [\[CrossRef\]](#)
4. Cheng, Z.; Lu, Z. Research on load disturbance based variable speed PID control and a novel denoising method based effect evaluation of HST for agricultural machinery. *Agriculture* **2021**, *11*, 960. [\[CrossRef\]](#)
5. Wan, L.; Dai, H.; Zeng, Q.; Sun, Z.; Tian, M. Characteristic analysis and co-validation of hydro-mechanical continuously variable transmission based on the wheel loader. *Appl. Sci.* **2020**, *10*, 5900. [\[CrossRef\]](#)
6. Dai, H.; Wan, L.; Zeng, Q.; Lu, Z.; Sun, Z.; Liu, W. Method and Test Bench for Hydro-Mechanical Continuously Variable Transmission Based on Multi-Level Test and Verification. *Machines* **2021**, *9*, 358. [\[CrossRef\]](#)
7. Zhu, Z.; Sheng, J.; Zhang, H.; Wang, D.; Chen, L. Optimization of Mode-Switching Quality of Hybrid Tractor Equipped with HMCVT. *Appl. Sci.* **2024**, *14*, 6288. [\[CrossRef\]](#)
8. Zhou, H.; Wang, L.; Lu, Z.; Qian, J.; Zhang, H.; Zhao, Y.; Cheng, Z.; Wang, X. Transmission Parameter Design and Characteristic Analysis of Three-Row Parallel Planetary Gear HMCVT. *Machines* **2022**, *10*, 740. [\[CrossRef\]](#)
9. Liu, X.J. *Analysis of Vehicle Transmission System*; National Defence Industry Press: Beijing, China, 1998; pp. 258–259.
10. Li, J.; Zhao, Y.; Zhai, Z.; Han, B.; Du, Y.; Wang, L.; Zhu, Z. Research on Design and Analysis Method of the Double Planetary HMCVT Based on High Efficiency Transmission. *Agriculture* **2022**, *12*, 1958. [\[CrossRef\]](#)
11. Zhang, G.; Zhang, H.; Ge, Y.; Qiu, W.; Xiao, M.; Xu, X.; Zhou, M. Mechanical Efficiency of HMCVT under Steady-State Conditions. *Shock Vib.* **2021**, *2021*, 4275922. [\[CrossRef\]](#)
12. Lu, K.; Liang, J.; Liu, M.; Lu, Z.; Shi, J.; Xing, P.; Wang, L. Research on Transmission Efficiency Prediction of Heavy-Duty Tractors HMCVT Based on VMD and PSO-BP. *Agriculture* **2024**, *14*, 539. [\[CrossRef\]](#)
13. Cheng, Z.; Lu, Z.; Qian, J. A new non-geometric transmission parameter optimization design method for HMCVT based on improved GA and maximum transmission efficiency. *Comput. Electron. Agric.* **2019**, *167*, 105034. [\[CrossRef\]](#)
14. Cheng, Z.; Zheng, S.; Qian, Y.; Lu, Z.; Zhang, H. Based on improved SA and GA a new method for optimizing transmission parameters of automotive HMCVT. *J. Mech. Strength* **2020**, *42*, 61–66.
15. Cheng, Z.; Chen, Y.; Li, W.; Liu, J.; Li, L.; Zhou, P.; Chang, W.; Lu, Z. Full factorial simulation test analysis and I-GA based piecewise model comparison for efficiency characteristics of hydro mechanical CVT. *Machines* **2022**, *10*, 358. [\[CrossRef\]](#)
16. Li, J.; Zhai, Z.; Song, Z.; Fu, S.; Zhu, Z.; Mao, E. Optimization of the transmission characteristics of an HMCVT for a high-powered tractor based on an improved NSGA-II algorithm. *Proc. Inst. Mech. Eng. Part D J. Automob. Eng.* **2022**, *236*, 2831–2849. [\[CrossRef\]](#)
17. Looman, J. *Zahnradgetriebe: Grundlagen, Konstruktionen, Anwendungen in Fahrzeugen*; Springer Science & Business Media: Berlin, Germany, 2009.
18. Rao, Z. *Planetary Gear Transmission Design*; Chemical Industry Press: Beijing, China, 2003.
19. Macor, A.; Rossetti, A. Optimization of hydro-mechanical power split transmissions. *Mech. Mach. Theory* **2011**, *46*, 1901–1919. [\[CrossRef\]](#)
20. Rossetti, A.; Macor, A. Multi-objective optimization of hydro-mechanical power split transmissions. *Mech. Mach. Theory* **2013**, *62*, 112–128. [\[CrossRef\]](#)
21. Xu, X.; Liang, Y.; Jordan, M.; Tenberge, P.; Dong, P. Optimized control of engine start assisted by the disconnect clutch in a P2 hybrid automatic transmission. *Mech. Syst. Signal Process.* **2019**, *124*, 313–329. [\[CrossRef\]](#)

**Disclaimer/Publisher’s Note:** The statements, opinions and data contained in all publications are solely those of the individual author(s) and contributor(s) and not of MDPI and/or the editor(s). MDPI and/or the editor(s) disclaim responsibility for any injury to people or property resulting from any ideas, methods, instructions or products referred to in the content.